A System for Simple Robotic Walking Assistance With Linear Impulses at the Center of Mass

Arash Mohammadzadeh Gonabadi, Prokopios Antonellis, and Philippe Malcolm, *Associate Member, IEEE*

***Abstract*— Walking can be simplified as an inverted pendulum motion where both legs generate linear impulses to redirect the center of mass (COM) into every step. In this work, we describe a system to assist walking in a simpler way than exoskeletons by providing linear impulses directly at the COM instead of providing torques at the joints. We developed a novel waist end-effector and high-level controller for an existing cable-robot. The controller allows for the application of cyclic horizontal force profiles with desired magnitudes, timings, and durations based on detection of the step timing. By selecting a lightweight rubber series elastic element with optimal stiffness and carefully tuning the gains of the closed-loop proportional–integral–derivative (PID) controller in a number of single-subject experiments, we were able to reduce the within-step root mean square error between desired and actual forces up to 1.21% of body weight. This level of error is similar or lower compared to the performance of other robotic tethers designed to provide variable or constant forces at the COM. The system can produce force profiles with peaks of up to 15 ± 2% of body weight within a root mean square error (RMSE) of 2.5% body weight. This system could be used to assist patient populations that require levels of assistance that are greater than current exoskeletons and in a way that does not make the user rely on vertical support.**

***Index Terms*— Aiding force, cable robotics, center of mass (COM), rehabilitation, walking.**

I. Introduction

THE field of wearable robots for assisting walking has witnessed an evolution from advanced, sophisticated devices that assist multiple joints [1]–[3] towards a greater focus on single-joint exoskeletons [4]–[9] and elegant, simple actuation mechanisms [10], [11]. A similar trend toward simpler interfaces and controls appears to be successful in the closely related field of exoskeletons for industrial applications [12]. In the present work, we describe an approach that is aimed at assisting walking in an even simpler way than single-joint assistance using timed linear impulses at the center of mass (COM).

Walking can be modeled as a motion whereby the COM moves over the stance leg, similar to an inverted pendulum [13]. This inverted pendulum motion requires almost no energy input during the single stance phase due to the efficient interchange between kinetic and potential energy [14]. However, energy input from ankle push-off is needed to redirect the COM from the downward phase of one step to the upward phase of the next step. Many exoskeletons and robotic prostheses are designed to mimic push-off [4], [10], [15], and we are starting to see different clinical applications for ankle exoskeletons [16]–[18], but there are many other ways to assist walking, such as assisting the knee [17], [19], the hip [5], [6], or even providing linear forces to the COM as in the inverted pendulum model.

Foundational studies from Gottschall and Kram [20] and others [21], [22] show that it is possible to reduce the metabolic cost of walking on a treadmill by up to 47% using an elastic tether that provides constant forward forces at the waist. Even though this type of device cannot be used for portable mobility assistance, assisting at the COM could be important for treadmill exercise therapy since the metabolic cost reductions are nearly twice as large as those with current exoskeletons [6], [8]. Gotschall and Kram [20] suggested that a future research direction could involve developing devices that allow assisting specifically during the propulsion.

Recently, there have been multiple new devices that can apply forces during specific portions of the gait cycle. A research group from Columbia University developed different multi-cable systems that can apply forces and moments in different directions at the pelvis [23]–[26]. A motorized version of their system can apply a net force that dynamically tracks the direction of the ground reaction force of the legs and could be used to elicit certain desirable compensatory after-effects when the device is turned off in individuals with hemiparesis [24]. Simha *et al.* [22] developed a robotic system with two tethers that can apply net forward or backward horizontal forces at the waist, and that can rapidly adjust the force levels from step to step. This device was used to artificially alter the relationship between step frequency and metabolic

Manuscript received December 2, 2019; revised March 9, 2020 and April 8, 2020; accepted April 13, 2020. Date of publication April 27, 2020; date of current version June 5, 2020. This work was supported in part by the Center for Research in Human Movement Variability, University of Nebraska at Omaha, in part by the National Institutes of Health under Grant P20GM109090, and in part by the Nebraska Established Program to Stimulate Competitive Research (EPSCoR) First under Grant OIA-1557417. The work of Prokopios Antonellis was supported in part by the University of Nebraska at Omaha, through a Graduate Research and Creative Activity (GRACA) Grant, and in part by the Advanced Mechanical Technology Inc (AMTI) Force and Motion Foundation. *(Corresponding authors: Arash Mohammadzadeh Gonabadi; Philippe Malcolm.)*

The authors are with the Department of Biomechanics, University of Nebraska at Omaha, Omaha, NE 68182 USA, and also with the Center for Research in Human Movement Variability, University of Nebraska at Omaha, Omaha, NE 68182 USA (e-mail: amgonabadi@unomaha.edu; pmalcolm@unomaha.edu).

This article has supplementary downloadable material available at http://ieeexplore.ieee.org, provided by the authors.

Digital Object Identifier 10.1109/TNSRE.2020.2988619

cost [27], which could be useful for exercise therapy. Bhat *et al.* [28] conducted experiments with relatively short and stiff tethers attached to a fixed anchor to elicit cyclic force profiles within every step as a result of small forward and backward movements on the treadmill. They found smaller reductions in metabolic cost compared to studies that use longer and less stiff tethers that were designed to maintain forces at a constant level [20], [21]. Penke *et al.* [29] developed another passive device that creates force profiles that rise and drop every stride using a pulley system that connects the waist to the movement of one of the ankles. They were able to reduce the metabolic cost of individuals poststroke by 12%, demonstrating the potential impact of timed force profiles in patient populations.

Simple models [13] and experiments with exoskeletons [7], [8], [30]–[32] show that actuation parameters such as the timing of force profiles can affect the impact of wearable robots. Differences in reductions in metabolic cost between studies with tethers that apply constant forces [20], [21] and tethers that apply cyclic forces once per step [28] or once per stride [29] confirm that assistance timing might also be important when using linear forces at the COM. Although passive systems have the benefit of being convenient to use (not requiring electromechanical hardware), a limitation of the existing studies with passive systems designed to produce cyclic forces is that they could not rigorously control the timing or other actuation parameters.

Our goal was to develop a robotic system that would allow applying cyclic horizontal force profiles with desired timings and magnitudes. A robotic system allows specifying actuation parameters, including timing and magnitude, and opens up new possibilities such as altering the actuation while the user is walking. However, it requires programming a control algorithm that is capable of applying desired force profiles with high repeatability. We hypothesized that a local optimum in force tracking performance could be achieved by varying the stiffness of a series elastic element in the transmission and by tuning the control algorithm gains. In the following sections, we present the system design, the optimization of the force tracking, and the evaluation of the system performance as well as a case study of the biomechanical response to demonstrate the feasibility of this system to guide application-specific hardware and software design of waist tethers for cable robots used in gait assistance and rehabilitation.

II. Methods

A. Actuation, Transmission, Interface

We developed a system [33], [34] based on an existing cable actuation unit and control platform (HuMoTech, Pittsburgh, PA, USA; Fig. 1, Movie 1) that is designed to enable scientists and clinicians to conduct studies with various prostheses and wearable robot end-effectors including exoskeletons and a harness. Since this is a commercially available platform, this work could enable other groups to reproduce similar experiments for different applications. The actuation unit generates forces using a direct-drive rotary motor (maximum speed: 4.98 ms^{-1}; maximum force: 6.58 kN). The actuator force is transmitted via a rope (diameter 3 mm, breaking strength 8.5 kN, Vectran, New England Ropes MA, USA). We designed a T-slotted pole

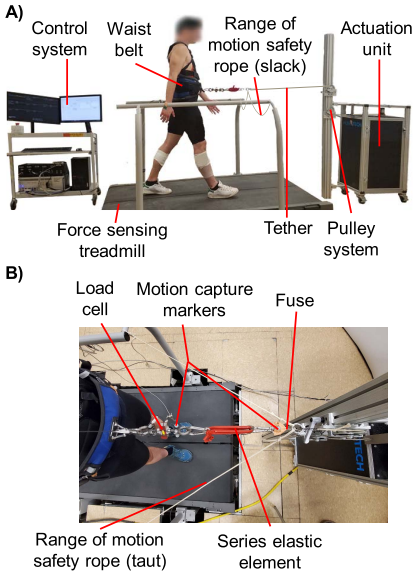

Fig. 1. System setup. A) Control station, actuation unit, tether, and waist belt. B) Tether close-up. The mechanical fuse consists of a double loop of fishing line with a tested breaking strength of ~350 N. The range of motion safety rope consists of a rope that is attached to the handrails, which becomes taut and prevents further pulling when the participant is at the front of the treadmill.

with two pulleys to allow for adjusting the angle of the applied force by changing the pulley height from 0.83 to 1.62 m. The distance between the pulley and the participant is 1.25 m when the participant is in the middle of the treadmill. This distance is less than in the system from Simha *et al.* [22] (4.09 m), but it was sufficient to keep the variation of the angle of the tether within a standard deviation of 0.9° (measured using motion capture) during walking, which is within range of another tether study (2° in [21]). The forces are applied to the person using a waist belt that is positioned such that the attachment point is at the height of the COM (at ~55% of body length in male participants [35]). We added a series elastic element to the tether to optimize the controller performance [36]–[38]. To ensure safety, we added a mechanical fuse that consists of fishing line (Trilene, Columbia, SC, USA).

B. Sensing and Controls

Ground reaction forces of both legs were measured at a rate of 1000 frames per second using a split-belt force treadmill (Bertec, Columbus, OH, USA). The tether forces were measured at a rate of 1000 frames per second using a tension load cell (Futek, Irvine, CA). The load cell was mounted at the attachment point with the participant to avoid underestimating or overestimating the applied forces due to oscillating mass from the tether components (elastic element or mechanical fuse). Certain cable robot studies use a similar configuration [21], [23], [39], and others appear to position load cells away from the participant [24], [25], [28] or estimate the forces based on the elongation of a spring [22]. The control station consists of an input-output interface (HuMoTech) and a real-time computer (SpeedGoat, Liebefeld, Switzerland) that runs a controller in Simulink (MathWorks, Data 1).

We developed a new high-level controller that is designed to apply sinusoidal tether force profiles with a desired onset

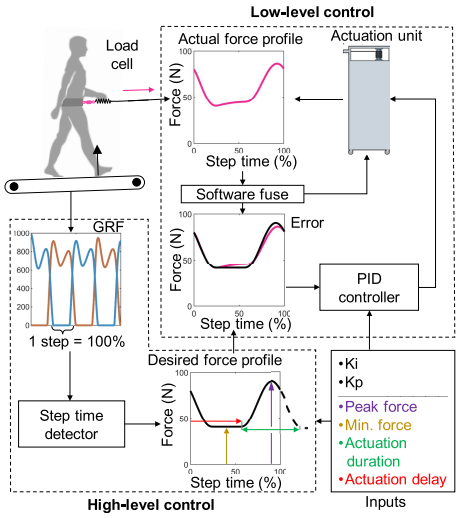

Fig. 2. Control flowchart. The high-level controller allows for specifying desired tether force profiles as a function of step time. Each step cycle begins with a heel strike of one leg and ends with the next heel strike of the opposite leg (the controller combines GRF data from both legs to calculate every desired force profile). The low-level controller adjusts the motor velocity to track the desired force profiles.

timing and duration (as a function of step time), and a desired minimum force and peak force magnitude (Fig. 2). Since the tether applies force to the COM, both legs are influenced by the system, and thus, it is not possible to control the left-right force distribution. Therefore, we chose to apply force profiles as a function of step cycle percentage instead of stride cycle percentage. The controller allowed force profiles that extend into the next step. Studies with exoskeletons have shown benefits of actuation profiles that begin before the contralateral heel strike and end after the contralateral heel strike [8]. As such, it might be beneficial to have the option of using force profiles that extend across the step transition.

The timings of the left and right heel strikes are detected based on the vertical ground reaction force using an adjustable detection force threshold set to 20 N. Since it is not possible to predict exactly when an ongoing walking step will end, the percentage of the step time is estimated based on the timing of the most recent heel contact and a moving average of three steps. This number could be reduced to one step for experiments where the controller has to follow rapid changes in step time. If the current step time falls inside the actuation period, the desired force will be the force of the programmed sinusoidal profile at the current step time percentage. If the current step time falls outside of the actuation period, the desired force will be the minimum force. In order to avoid undetected steps, we instructed the participant to keep his feet on the corresponding sides of the split-belt treadmill, and the controller only registered heel strikes after a toe-off was detected (using a 20 N threshold). The real-time force profiles and the sound of the actuator unit were inspected to determine if errors occurred in the step detection. We did not notice any step detection errors in the single-subject experiments. The low-level controller, developed by HuMoTech, communicates with the motor and adjusts its velocity to minimize the error between the actual force, which is measured with the load cell, and the desired force by using a closed-loop proportional–integral–derivative (PID) algorithm with configurable gains [15]. In a PID controller, the proportional gain (Kp) adjusts the output proportionally to the error, which affects the rise time; however, using only a proportional gain can sometimes result in steady-state errors. The integral gain (Ki) adjusts the output as a function of the integral of the error, and while this can reduce overshoots, it can make the transient response worse. The derivative gain (Kd) increases the stability of the system, reduces the overshoot, and improves the transient response. Depending on the system behavior, sometimes it is not necessary to use all of the gains to control a system. We set the derivative gain, Kd, to zero in all experiments since pilot tests showed that using derivative control was not effective.

C. Safety Features

The safety requirements of using a waist tether connected to a high powered off-board actuation system can be expected to be similar to exoskeletons, exosuits, or prostheses tethered to a high powered off-board system [15], [40], [41] except for a number of differences. While exoskeletons and prostheses apply torques, the waist-tether applies linear forces. To eliminate the risk of falling, the person is secured with a ceiling harness (Petzl, Crolles, France). Exoskeletons often have a hard stop that limits the joint range of motion. To restrict the forward motion of a participant, we attached the end of the tether to the treadmill handrails with a limiter rope that had a breaking strength that is ~30 times greater than the mechanical fuse. The length of the limiter rope was set to be slack during normal walking, but it would become taut and prevent further forward movement of the person to the front-end of the treadmill.

To minimize risks due to excessive forces and accelerations, we used three additional safety features. A remote stop button allows for stopping the motor when the participant or the experimenter detects an issue. A limit setting in the software (software fuse), stops the motor when the load cell force exceeds 300 N. We designed a mechanical fuse consisting of two loops of fishing line (Trilene) that disconnects the tether if the force increases above the breaking strength. We first tested the mechanical fuse by applying a slow (quasi-static) increasing force on one loop of the breakaway material. The results of repeated testing indicate that a single loop breaks at 147 ± 27 N (mean ± standard deviation), which falls below the advertised (nominal) breaking strength (178 N for one loop). Next, we conducted a test where we applied a sinusoidal force profile as during walking (Movie 2). In this test, a single loop broke at 135 ± 20 N. Altogether, these tests confirmed that the mechanical fuse consistently breaks below the nominal breaking strength with a low standard deviation (around 5% of body weight (BW) for a 70 kg person). During walking experiments with healthy adult participants, we normally use two loops of the mechanical fuse which restricts the peak forces to about 350 N. This allows us to apply forces up to a range that falls within the range of horizontal forces that humans are capable of producing during fast walking [42]. This mechanical safety system has the advantage that it is

robust to software or force sensing failures. A similar system could potentially be useful in other cable-rehabilitation robots.

D. Optimization and Evaluation Protocol

We conducted a number of single-subject analyses to select the human-device interface (waist belt), the series stiffness, antagonistic force level, and the PI gains, and to evaluate the similarity to normal walking, the responsiveness, and the range of force profiles (Data 2). We acknowledge that this approach (conducting multiple experiments on a single participant) is different from the typical approach of a hypothesis-driven study where one experiment is conducted in multiple participants. Similar to a number of studies that introduce new assistive devices [38], [43], [44], our goal of this manuscript was not to describe the human adaptation but to optimize and evaluate a new system for future experiments (similar to [38], [43], [44]). We conducted multiple analyses of walking recordings on data from one healthy male participant (age 28 yrs, mass 83 kg, height 1.81 m). The experiments were approved by the Institutional Review Board of the University of Nebraska Medical Center, and the participant provided informed consent. Since the system is composed of passive elements (e.g., springs) and algorithms that behave in a repeatable way, it is assumed that the relative results from the device sensor measurements from single-subject experiments can be reproduced in other participants but at different absolute values [38]. As such, single-subject experiments can provide useful information about the system performance; however, we acknowledge that further experiments are needed to more completely understand the human response results.

E. Analyses

We evaluated the force tracking by calculating the root-mean-square of the error (RMSE) between the actual and desired force. To understand how well the system tracks the force profiles within a step, we calculated the results of the RMSE of the actual and desired force time series of each step. Furthermore, to assess how well the system tracks the average force per step, we reported the RMSE of the average force per step [22]. To detect undesirable high-frequency oscillations, we calculated the oscillation-level metric proposed by Zhang and Collins *et al.* [38]. This metric is obtained by high pass filtering the error with a 10 Hz cut-off frequency, followed by taking the integral of the energy spectral density. All analyses were conducted in MATLAB (MathWorks, Natick, MA, USA).

III. Hardware Optimization

A. Human Interface (Waist Belt) Selection

During pilot testing, we surmised that the sinusoidal force profiles imposed additional demand on the abdominal musculature to maintain trunk alignment. We conducted a test comparing a resistance training waist belt (SKLZ, Durham, NC, USA) to a waist belt that is designed specifically for sporting activities that involve abrupt changes in forces (kiteboarding; Mystic boarding, Katwijk aan Zee, Netherlands). We refer to the resistance training waist belt as the α-waist belt and the kiteboarding waist belt as the β-waist belt. We measured the muscle activation of the rectus abdominis (Trigno Avanti, Delsys, USA; 2000 Hz) in one participant during four walking trials of one minute each at 1.25 ms^{-1}. In each trial, we applied a tether force profile with a minimum force of 5% BW (39 N), a peak force of 17% BW (136 N), onset time at 56% of the step, and an actuation duration of 66% of the step (i.e., the force profile started during the second half of the step and continued until 122% which corresponds to 22% of the next step). Both belts were tested with a (previously tuned) proportional gain (Kp) set to a value of 8, an integral gain (Ki) set to 0, and a series elastic element with a 1748 Nm^{-1} stiffness (6 loops of red Thera-Band latex tubing resulting in a slack length of each closed-loop of about 14 cm; Akron, OH, USA). To limit the order effects, we used a reverse counterbalancing (ABBA) randomization order whereby the participant wore the α-waist belt (during the first and last trial), and during the second and third trials, he wore the β-waist belt. The results of this case study suggest that the larger back support of the β-waist belt could induce a small reduction in trunk flexor muscle activation (Fig. 3B). The mean reduction was very small ($\sim$ 1%) and the activity level of the analyzed muscle was very low compared to the maximum voluntary contraction (MVC), thus the observed reduction is not clinically relevant. Additional electromyography (EMG) measurements (e.g., targeting deeper muscle layers that are more important for trunk stabilization) or comfort-related measurements (pressure, skin temperature, skin redness, comfort questionnaires) could provide further information about the human-device interface. As with the other single-subject experiments in this study, additional validations should be performed to determine whether this result is consistent across participants and how the potential comfort benefit weighs against the greater mass of the β-waist belt (2.15 kg vs. 0.31 kg).

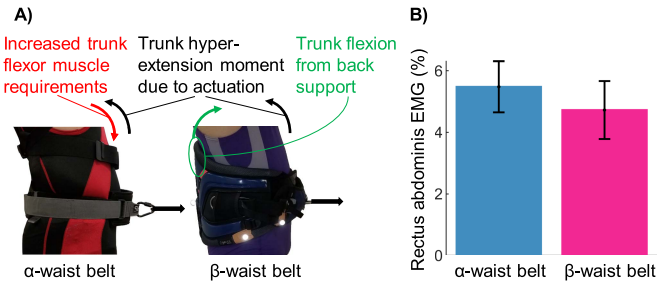

Fig. 3. Human interface (waist belt) comparison. A) α and β waist belt prototypes. B) Mean rectus abdominis EMG of one participant in percent of MVC. Error bars show the standard deviation between steps. (n $\approx$ 200 steps per condition).

B. Series Elastic Element Stiffness Optimization

It is known that series elasticity affects actuator control performance [36]–[38]. High stiffness allows faster response times, but it could generate noise, while intermediate stiffness can improve force tracking or minimize motor requirements by storing and releasing energy though it could introduce delay. Studies with tethers designed for applying constant forces use

long elastic elements with low stiffness [20], [45], [46] such that changes in the position on the treadmill have negligible effects. Studies with dynamic tethers use series elastic elements that provide a compromise between low sensitivity to changes in position on the treadmill and sufficient force bandwidth. To identify the optimal stiffness, we conducted an experiment with a range of stiffnesses that were obtained by combining multiple 14 cm loops of red Thera-band in parallel. We also tested two stainless steel springs. All conditions were tested under the same settings as the waist belt selection test except for the PI gains, which were tuned for every series elastic stiffness condition. We included an additional healthy male participant (age 40 yrs, mass 84 kg, height 1.80 m) for this test (referred to as participant 2) to verify that trends in system parameters can be consistent across participants. The spring stiffnesses were calculated by plotting the force measured with the load cell versus the series elastic element elongation measured with motion capture markers attached to steel rings that were used to connect both ends of the elastic element to the tether (VICON Vero, Oxford Metrics, Yarnton, UK; 100 Hz). The values on the horizontal axis in Fig. 4 are based on force and length changes during walking experiments. In addition, we measured the stiffness in quasi-static tests where the elastic element was moved through its range of elongation. Results showed that the within-step RMSE reaches a minimum at 3000 and 2500 Nm^{-1} in participants 1 and 2, respectively. However, the between-step RMS starts rising after ~2500 Nm^{-1} with higher stiffnesses, and the oscillation level also increased with higher stiffnesses, resulting in an ideal stiffness range for the different error measurements between 2500 and 3000 Nm^{-1} (Fig. 4).

The optimal stiffness appears to be of a similar order of magnitude as stiffnesses used in other cable robots (2280 Nm^{-1} in [23]; 2500 Nm^{-1} in [24]). Interestingly, the steel spring with the highest stiffness (2577 Nm^{-1}) resulted in a within-step RMSE that was approximately twice as high as the Thera-band spring with equivalent stiffness. Quasi-static stiffness tests showed that the Thera-band has a non-linear stiffness and hysteresis (Fig. 5A). A study on optimal control for exoskeletons suggests using a "damping-injection" term that limits changes in motor velocity as a way to reduce errors [47]. While our PI-controller did not include the damping-injection term, it is possible the hysteresis from the Thera-band springs contributed to better force tracking. Perhaps similar non-steel springs with low weight and high hysteresis could be beneficial in other rehabilitation robots with long suspended cables [22], [26], [39], [48].

It might be possible that results for these types of experiments can be predicted by theoretical or numerical models [49], [50]. Zhang *et al.* [38] showed that a series elastic stiffness that matches the slope of the desired force versus displacement is optimal for emulating elastic exoskeletons. Our optimized series elastic stiffness did not match with this hypothesis (Fig. 5B). This is not surprising since our desired actuation profile was a time-based profile and could not be mimicked with a spring.

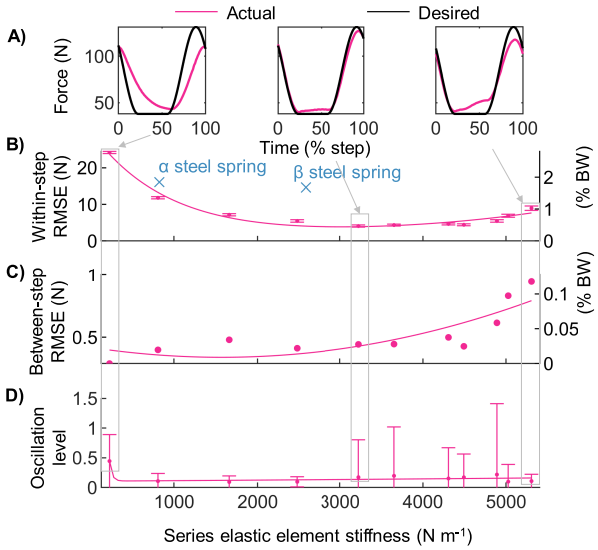

Fig. 4. Series elastic stiffness optimization. A) Desired tether force (black) and actual tether force (magenta) of walking with different series elastic element stiffnesses. B) Within-step RMSE versus stiffness. Dots and error bars represent the mean and standard deviations of the steps of the tested Thera-band conditions. Blue crosses represent results from two stainless steel springs. The magenta lines represent curve fits. C) Between-step RMSE. This result is the RMSE in the average force per step, as in [22]. D) Signal oscillation level. This represents the amount of high-frequency noise and is calculated as in [38]. (n ≈ 50 steps per condition).

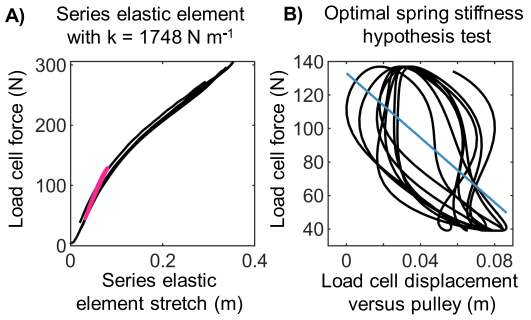

Fig. 5. Series elastic stiffness characterization. A) Stiffness calculation from the condition with k = 1748 Nm^{-1} in Fig. 4A. The black line represents force and displacement measurements while slowly moving the series elastic element through its range of motion. The magenta line shows behavior during walking from which the stiffness was obtained. B) Test of optimal series stiffness hypothesis from Zhang *et al.*, [8]. The black line shows the desired tether force versus anterior-posterior displacement of the attachment point of the waist belt. The blue line represents a linear fit. The linear fit has a negative slope (lower force with greater elongation and vice versa), which means that the behavior could not be mimicked with a physical spring.

C. Antagonistic Force Optimization

To test predictions from simple models on the effects of impulses acting at the COM, we wanted to have the capability to apply short force bursts of net forward forces. However, it would be challenging for the force-controller to transition to and from phases where the cable goes slack. To avoid such discontinuities, different cable-robot systems use two antagonistic force cables such that one can apply a net-zero force by providing a certain baseline force with one cable [51]. We chose to simulate a constant backward force by inclining the treadmill, similar to another study [27]. To obtain

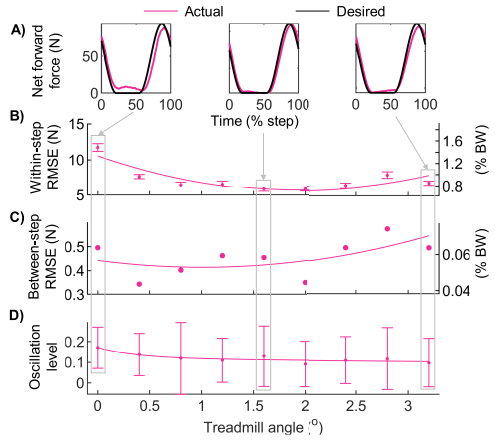

Fig. 6. Antagonistic force optimization. A) Desired net forward force (black) and actual net forward force (magenta) of walking with different antagonistic force levels produced by different treadmill inclinations. The net forward force profile was kept constant in all conditions by matching the increases in antagonistic force from the treadmill inclination with the increases in tether force. B) Within-step RMSE. C) Between-step RMSE. D) Signal oscillation level. (n ≈ 100 steps per condition).

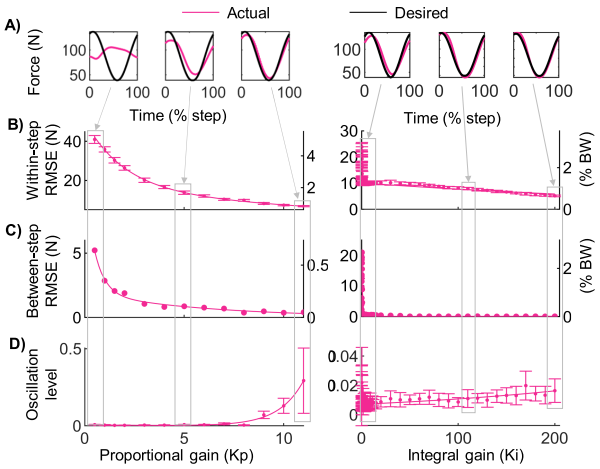

Fig. 7. Gain tuning. A) Desired tether force (black) and actual tether force (magenta) of walking test with different proportional and integral gains. B) Within-step RMSE versus Kp and Ki. Dots and error bars represent the mean and standard deviations of the steps. C) Between-step RMSE. D) Signal oscillation level. (n ≈ 22 and 11 per condition for Kp and Ki sweep).

a net-zero force, we then applied a tether force equivalent to the tangential component of gravity. We assessed different antagonistic force levels using the same net forward force profile with the settings from the waist belt selection test but with tuned gains for each condition in one participant (Fig. 6). The results confirm that not using an antagonistic force leads to increased errors due to tether oscillations. Increasing the treadmill grade reduced the oscillation level and reduced the within-step RMSE until a treadmill grade of 2°, which corresponds to an antagonistic force level of 3.5 % BW. In all other tests, we used a treadmill inclination of 3°, which produced an antagonistic force level of 40 N that was similar to the antagonistic force level used in another cable robot [39]. The optimal force level is likely dependent on the tether components. A lighter tether would require smaller antagonistic forces to keep the tether taut and vice versa. Our tether weighed 0.35 kg (mass of load cell, elastic element, mechanical fuse, carabiners, and rest of tether), which explains the need for a 40 N antagonistic force.

IV. Gain Tuning

Tuning a waist tether can potentially be more challenging than tuning an exoskeleton or prosthesis because the forces are highly sensitive to changes in the position on the treadmill. Some studies use open-loop algorithms that apply a certain predefined output (e.g., spring compression) instead of minimizing the error between the desired forces and load cell measurements [22], [39]. For closed-loop PID algorithms, it is possible to manually tune the gains or to use an automatic tuning algorithm. With wearable exoskeletons, it seems common to use manual tuning [17], [47]. We manually tuned the gains, but we used a consistent tuning strategy whereby we tuned Kp first while keeping Ki at zero, followed by tuning Ki, to avoid that the tuning order would affect the results. We conducted a parameter sweep where we varied Kp from 0.5 to 11 while keeping Ki at 0, followed by another sweep where we varied Ki from 0 to 200 while keeping Kp at 8. In both experiments, we tested the same participant using the same onset time and peak force settings as in the waist belt selection experiment. By tuning Kp and Ki, we were able to reduce the within-step RMSE to 1.21 % BW (9.87 N), the between-step RMSE to 0.05% BW (0.38 N) and the oscillation level to 0.005, at a Kp of 8 and Ki of 0 (Fig. 7). These minimized RMSE values appear to be slightly lower than the results of a system that changes forces once per step by Simha *et al.* [22] (within-step RMSE 2.64%, between-step RMSE 0.39% BW).

Our values appear to fall within the range of errors in anterior-posterior forces obtained from studies with cable robots (within-step RMSE 2% BW in [23], [25], and 0.92% BW in [24]). Another point of comparison is the study from Grabowski and Kram [52] that describes an elastic tether with a rudimentary but elegant force indicator for manually towing a person during running. They report that it is possible to maintain a constant force within a range of 2 N. It appears that our waist-tether and similar robotic devices from others currently do not match the accuracy of this manual device. Of course, tracking a dynamic force profile would be more challenging with a manual system. As already described [22], we found that the gains need to be tuned for individual participants. In the tuning sessions from an experiment with 10 participants [34], we found that the best Kp was around 7.72 ± 2.22, whereas the best Ki was 3.57 ± 15.70 (mean ± standard deviation). To facilitate future experiments, we plan to work on automating the tuning process.

V. System Performance Evaluation

A. Similarity to Normal Walking

To avoid that the tether goes slack during portions of the force profile where the desired net forward force is zero, we simulated an antagonistic force by inclining the treadmill by 3° and applied a constant tether force of 5% BW to offset the backward parallel component of gravity due to the treadmill inclination. Without this constant tether force

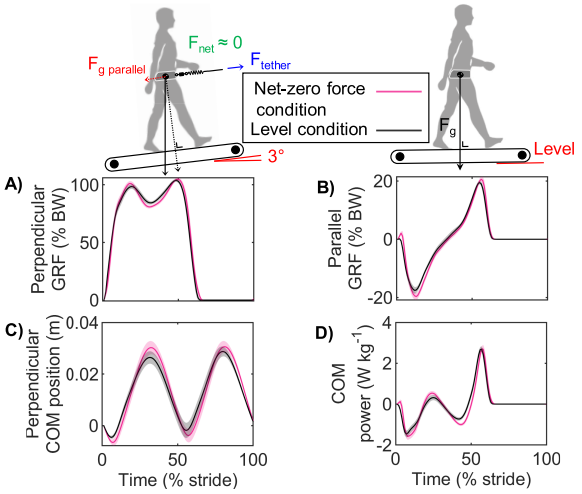

Fig. 8. Comparison of kinetics and kinematics during the net-zero force condition and untethered level walking. A) Perpendicular ground reaction force. B) Parallel ground reaction force. C) Perpendicular COM position. COM position was obtained by double integrating the total perpendicular force from the treadmill (and the tether) [54]. D) COM power. Individual leg power was calculated using the method from [55] (n ≈ 100 steps per condition).

of 5% BW, a 3° inclination would be sufficient to alter the kinematics and kinetics of walking compared to level walking [53]. To verify how well the tether force from the net-zero force condition makes walking similar to level treadmill walking without a tether, we compared whole-body kinetics and kinematics in one participant during walking under both conditions at 1.25 ms^{-1}. The results indicate that the gait kinetics and kinematics were similar, which shows that this setup can mimic normal walking (Fig. 8).

B. Responsiveness

We evaluated the system's responsiveness by measuring the rise time to achieve 90% of a desired change in force. We conducted an experiment with one male participant who walked at 1.25 ms^{-1} while we gradually reduced the desired force duration from 100 to 5% of the step. All the other settings were kept constant at the settings of the waist belt selection experiment. We observed the fastest rise time interval of 0.013 ± 0 s resulting in a force rate of 4187 ± 30 Ns^{-1} (mean ± standard deviation) in the 5% actuation duration condition (Fig. 9).

Simha *et al.* [22] reported an average force rate of 5188 Ns^{-1} during an experiment in which their tether was attached to a fixed anchor. Our system was able to approach this force rate under more challenging conditions where the tether was attached to a human. Our drop times were the fastest in the 5% actuation duration condition; however, they were about twice as slow as the rise times (2195 ± 167 Ns^{-1}). This could be due to the actuator having to suddenly reverse its velocity after increasing the force and the movement of the participant.

To obtain an idea of the responsiveness independent of the movement of the participant, we conducted a bandwidth test where the tether was attached to a fixed anchor (Movie 3). We applied a sinusoidal tether force profile with the same magnitude settings, series stiffness, and gains as the previous

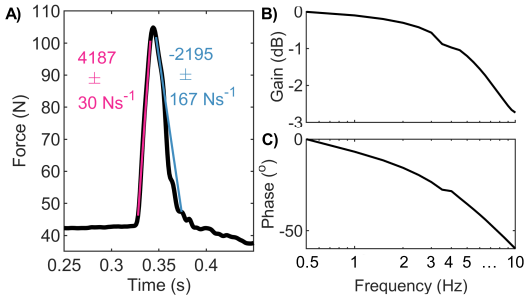

Fig. 9. Responsiveness. A) The black line indicates a representative tether force profile with a 5% duration. The magenta line represents the slope from 5 to 95% of the peak. The blue line represents the slope of a drop from 95 to 5%. Numbers represent mean ± standard deviation of all steps (n ≈ 17 steps per condition). B) Gain plot of fixed-endpoint bandwidth test. C) Phase plot of the bandwidth test. (n = 829 steps).

experiments over a range of simulated step frequencies from 0.5 to 10 Hz. The results show that the system has a 3 dB cutoff of about 10 Hz and a 60° phase delay at 10 Hz. The 3 dB cutoff is higher than the tether system from Brown *et al.* [39], similar to an ankle tether system from Wu *et al.* [56] but lower than high-performance exoskeletons and prostheses [15], [44]. Since the majority of normal walking movements occur below 6 Hz, this confirms that the system is fast enough to track and assist walking. The fact that the RMSE values were within the range of existing systems (section IV) and that the bandwidth was higher than the frequency range of walking suggests that the elastic element length adequately struck a balance between accuracy and responsiveness. We found a 60° phase delay at 10 Hz, which is on the lower side of the range of phase delays reported in studies with robotic tethers and exoskeletons (i.e., 45° to 90° in [44], 85° in [15], 145° in [39]). In future experiments, this delay could potentially be corrected by using an iterative learning controller [47] that measures how much the actual force profile is delayed compared to the desired force profile over a number of steps and then shifts the motor commands in order to correct for the delay.

C. Feasible Range of Actuation Profiles

To evaluate the range of achievable profiles, we conducted an experiment where one participant walked under 32 different force profiles with peak times ranging from 0 to 100% of the step, durations ranging from 33 to 100% of the step and peak net forward forces ranging from 30 N to 184 N (3 to 23% BW). All other settings were the same as in the waist belt selection experiment. The gains were manually tuned. We investigated which force profiles could be obtained with a within-step RMSE of 2.5% BW or lower. We chose this threshold based on within-step RMSE values that appear acceptable in the literature [22], [24]. The results indicate that it is possible to apply actuation profiles up to peak net forces ranging from 11 to 17% BW with a within-step RMSE below 2.5% BW (Fig. 10). The range of forces that can be applied within this RMSE appears of a similar order of magnitude as the maximum forces reported from another study with a cable robot (157N, [25]). When we consider walking relative to a reference system that moves with the treadmill belt, peak net forward forces up to 184 N applied to a person walking at 1.25 ms^{-1}, provide a power of 230 W to the person.

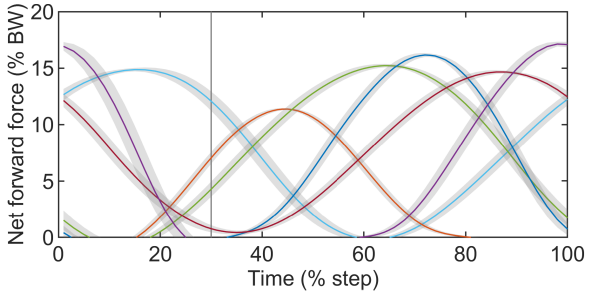

Fig. 10. Range of force profiles. Examples of net forward force profiles that could be achieved with a within-step RMSE lower than 2.5% BW. Lines and shaded regions represent the mean and standard deviation of consecutive steps (2 min. per condition). Net forward force profiles with higher and lower peak forces were tested at every timing (from 3 to 22% BW). For each timing, we only plotted the highest force profile that could be achieved within the within-step RMSE threshold. (n ≈ 107 steps per condition).

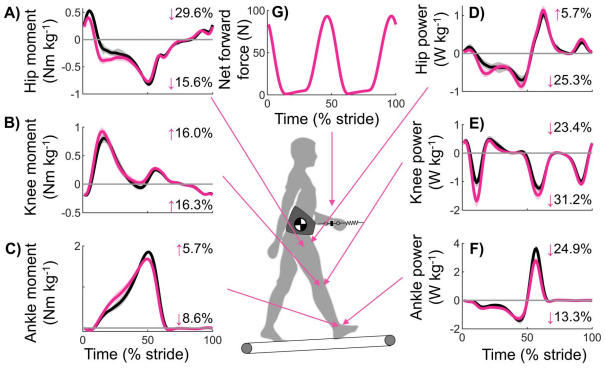

Fig. 11. Biomechanical results. Analysis of joint kinetics in one participant. Magenta lines represent walking with the force profile of the waist belt optimization test. Black lines represent walking with the net-zero force condition. Positive and negative moments indicate extension and flexion, respectively. Positive and negative powers indicate generation and adsorption, respectively. Percentages indicate percent change in stride-averages of positive and negative portions (n ≈ 100 strides).

VI. Biomechanical Tests

To evaluate the effects of our system on human walking, we analyzed the effects of one force profile on a number of commonly evaluated joint kinetic metrics. We processed motion capture data (VICON) of the participant from the waist belt selection protocol under the same force profile using OpenSim (SimTK, Santa Clara County, California, USA). The force profile resulted in the largest reduction in stride average of the moment at the hip (29.6% in hip extension moment; Fig. 11A), but led to increases in the extension moment of the ankle and knee joints (5.7% and 16%, respectively; Fig. 11 C, B). The force profile also reduced positive ankle and knee joint power (by 24.9% and 23.4%, respectively; Fig. 11 F, E), but it increased positive hip power (by 5.7%; Fig. 11D) and all negative joint powers (by percentages ranging from 13.2% to 25.3%). The force profile acted from 28 to 61% of the stride cycle (i.e., single stance and second double support) and from 78% of the stride to 11% of the next stride cycle (i.e., swing and first double support). These phases overlapped with the hip extension moment and positive power in the ankle and knee, which could explain why the system resulted in decreases in these kinetics. It is known that the human interaction to wearable robots results in adaptation over time and variability between participants; however, these preliminary results demonstrate the utility of our system on a human subject. Additional experiments with multiple subjects that explore the effects of alterations in system parameters (i.e., timing, magnitude) are necessary to fully understand human interaction with the device.

VII. General Discussion

This work describes a simple cable robot that can safely apply cyclic forward force profiles at the COM within a similar level of accuracy as other cable robots that apply constant [22], [48], or non-constant forces [23]–[25]. We obtained accurate force tracking by optimizing the PI gains and series elastic element stiffness. The range of the peak forces and peak assistive powers appear to be relatively high compared to similar cable robots [22], [24], [25], [56]. We performed single-subject experiments to provide proof-of-concept of the feasibility of our system performance that supports performing future experiments with multiple subjects to demonstrate the generalizability of the system in gait assistance and rehabilitation settings. While this robotic tether cannot be used for portable mobility assistance, we believe that the capacity to apply such high assistance magnitudes could be useful in patient populations that have high increases in metabolic cost (e.g., children with cerebral palsy have 200-300% increase in metabolic cost [57]). In these populations, traditional exoskeletons that can reduce the metabolic cost by up to about 25% [6], [8] might not be sufficient to unlock the potential benefits of walking exercise therapy at faster speeds [58] or with a higher dosage [59].

Optimal strategies for robot-assisted gait rehabilitation are still under investigation [60], [61]. Studies indicate that rehabilitation robots should not rigidly guide or support a patient's movement [62]–[64]. In this regard, a robotic waist tether that applies horizontal forces could be opportune since it can assist propulsion and reduce metabolic cost without providing any support in the vertical direction, thus demanding a continuous and strong engagement of the user. While constant horizontal forces can already reduce the metabolic cost of walking in healthy individuals by up to 47% [20], it could be hypothesized that optimized non-constant force profiles could allow greater reductions in patient populations with unsteady velocity (e.g., individuals with Parkinson's disease who encounter freezing [65] or individuals poststroke with asymmetric gait [66]). This hypothesis was confirmed by the study from Penke *et al.* [29] that showed greater reductions in metabolic cost in poststroke individuals using non-constant forces at the COM compared to using constant forces. It is plausible that an error augmentation strategy [60], [62], [67] could be more beneficial than only focusing on minimizing metabolic rate for gait rehabilitation protocols with a waist tether. In patients with asymmetric gait such as individuals poststroke, error augmentation could be achieved by providing impeding forces during paretic side propulsion or providing aiding forces during non-paretic side propulsion. The latter could possibly combine the advantages of error augmentation together with metabolic cost reduction, which could allow for longer training protocols.

Robotics, in general, has a trend towards anthropomorphic designs [68], and in wearable robotics, a lot of groups design bioinspired devices that assist at a joint level (e.g. [69]). While certain gait impairments require assisting specific joints, there might be cases where it could be more beneficial to act directly at the COM. Studies on individuals poststroke show that their increased metabolic cost can be explained by altered COM mechanics [70], [71]. It has been found that metabolic cost can be reduced by 30% in individuals poststroke when they are instructed to reduce their vertical COM displacement and when they are provided biofeedback of their vertical COM displacement [72].

Due to the high range and repeatability of achievable forces and changes in metabolic cost [34], robotic waist tether experiments could produce rich datasets for trend validation of musculoskeletal simulations and muscle-metabolic cost estimations [73]–[75] since it could be possible to achieve larger changes in metabolic cost compared to non-robotic perturbations such as footwear [76] or static tethers [20], [21]. While the robotic tether is fixed in a treadmill environment, experiments with this system could be used to emulate and optimize control strategies for mobile devices such as motorized rollators [77], [78], or even more exotic assistive devices such as a running jetpack [79]. Experiments with a robotic waist tether that allows for control with precise timing and magnitude could also be used to inform how to best manually assist patients.

Acknowledgment

The authors would like to thank A. Harp and M. Fritton for help with pilot testing, and B. Senderling, T. Vanderheyden, and HuMoTech for technical support. They would also like to thank J. Caputo for his constructive feedback on the manuscript draft and the anonymous reviewers for their suggestions for improving the manuscript.

References

[1] W. van Dijk and H. Van der Kooij, "XPED2: A passive exoskeleton with artificial tendons," *IEEE Robot. Autom. Mag.*, vol. 21, no. 4, pp. 56–61, Dec. 2014.

[2] A. Zoss and H. Kazerooni, "Design of an electrically actuated lower extremity exoskeleton," *Adv. Robot.*, vol. 20, no. 9, pp. 967–988, Jan. 2006.

[3] C. J. Walsh, K. Endo, and H. Herr, "A quasi-passive leg exoskeleton for load-carrying augmentation," *Int. J. Hum. Robot.*, vol. 04, no. 03, pp. 487–506, Sep. 2007.

[4] L. M. Mooney, E. J. Rouse, and H. M. Herr, "Autonomous exoskeleton reduces metabolic cost of human walking during load carriage," *J. NeuroEng. Rehabil.*, vol. 11, no. 1, p. 80, 2014.

[5] J. Kim *et al.*, "Reducing the metabolic rate of walking and running with a versatile, portable exosuit," *Science*, vol. 365, no. 6454, pp. 668–672, Aug. 2019.

[6] J. Lee, K. Seo, B. Lim, J. Jang, K. Kim, and H. Choi, "Effects of assistance timing on metabolic cost, assistance power, and gait parameters for a hip-type exoskeleton," in *Proc. Int. Conf. Rehabil. Robot. (ICORR)*, Jul. 2017, pp. 498–504.

[7] P. Malcolm, W. Derave, S. Galle, and D. De Clercq, "A simple exoskeleton that assists plantarflexion can reduce the metabolic cost of human walking," *PLoS ONE*, vol. 8, no. 2, 2013, Art. no. e56137.

[8] J. Zhang *et al.*, "Human-in-the-loop optimization of exoskeleton assistance during walking.," *Science*, vol. 356, no. 6344, pp. 1280–1284, 2017.

[9] B. T. Quinlivan *et al.*, "Assistance magnitude versus metabolic cost reductions for a tethered multiarticular soft exosuit," *Sci. Robot.*, vol. 2, no. 2, Jan. 2017, Art. no. eaah4416.

[10] S. H. Collins, M. B. Wiggin, and G. S. Sawicki, "Reducing the energy cost of human walking using an unpowered exoskeleton," *Nature*, vol. 522, no. 7555, pp. 212–215, Jun. 2015.

[11] R. Nasiri, A. Ahmadi, and M. N. Ahmadabadi, "Reducing the energy cost of human running using an unpowered exoskeleton," *IEEE Trans. Neural Syst. Rehabil. Eng.*, vol. 26, no. 10, pp. 2026–2032, Oct. 2018.

[12] M. P. de Looze, T. Bosch, F. Krause, K. S. Stadler, and L. W. O'Sullivan, "Exoskeletons for industrial application and their potential effects on physical work load," *Ergonomics*, vol. 59, no. 5, pp. 671–681, May 2016.

[13] A. D. Kuo, "Energetics of actively powered locomotion using the simplest walking model," *J. Biomechanical Eng.*, vol. 124, no. 1, pp. 113–120, Feb. 2002.

[14] G. A. Cavagna, N. C. Heglund, and C. R. Taylor, "Mechanical work in terrestrial locomotion: Two basic mechanisms for minimizing energy expenditure," *Amer. J. Physiol.-Regulatory, Integrative Comparative Physiol.*, vol. 233, no. 5, pp. R243–R261, Nov. 1977.

[15] J. M. Caputo and S. H. Collins, "A universal ankle–foot prosthesis emulator for human locomotion experiments," *J. Biomechanical Eng.*, vol. 136, no. 3, Mar. 2014, Art. no. 035002.

[16] L. N. Awad *et al.*, "A soft robotic exosuit improves walking in patients after stroke," *Sci. Translational Med.*, vol. 9, no. 400, Jul. 2017, Art. no. eaai9084.

[17] Z. F. Lerner *et al.*, "An untethered ankle exoskeleton improves walking economy in a pilot study of individuals with cerebral palsy," *IEEE Trans. Neural Syst. Rehabil. Eng.*, vol. 26, no. 10, pp. 1985–1993, Oct. 2018.

[18] K. Z. Takahashi, M. D. Lewek, and G. S. Sawicki, "A neuromechanics-based powered ankle exoskeleton to assist walking post-stroke: A feasibility study," *J. NeuroEng. Rehabil.*, vol. 12, no. 1, p. 23, 2015.

[19] M. K. MacLean and D. P. Ferris, "Energetics of walking with a robotic knee exoskeleton," *J. Appl. Biomech.*, vol. 35, no. 5, pp. 320–326, Oct. 2019.

[20] J. S. Gottschall and R. Kram, "Energy cost and muscular activity required for propulsion during walking," *J. Appl. Physiol.*, vol. 94, no. 5, pp. 1766–1772, May 2003.

[21] C. A. Zirker, B. C. Bennett, and M. F. Abel, "Changes in kinematics, metabolic cost, and external work during walking with a forward assistive force," *J. Appl. Biomech.*, vol. 29, no. 4, pp. 481–489, Aug. 2013.

[22] S. N. Simha, J. D. Wong, J. C. Selinger, and J. M. Donelan, "A mechatronic system for studying energy optimization during walking," *IEEE Trans. Neural Syst. Rehabil. Eng.*, vol. 27, no. 7, pp. 1416–1425, Jul. 2019.

[23] V. Vashista, X. Jin, and S. K. Agrawal, "Active tethered pelvic assist device (A-TPAD) to study force adaptation in human walking," in *Proc. IEEE Int. Conf. Robot. Autom. (ICRA)*, May 2014, pp. 718–723.

[24] V. Vashista, D. Martelli, and S. K. Agrawal, "Locomotor adaptation to an asymmetric force on the human pelvis directed along the right leg," *IEEE Trans. Neural Syst. Rehabil. Eng.*, vol. 24, no. 8, pp. 872–881, Aug. 2016.

[25] J. Kang, V. Vashista, and S. K. Agrawal, "On the adaptation of pelvic motion by applying 3-dimensional guidance forces using TPAD," *IEEE Trans. Neural Syst. Rehabil. Eng.*, vol. 25, no. 9, pp. 1558–1567, Sep. 2017.

[26] V. Vashista, S. K. Mustafa, and S. K. Agrawal, "Experimental studies on the human gait using a tethered pelvic assist device (T-PAD)," in *Proc. IEEE Int. Conf. Rehabil. Robot.*, Jun. 2011, pp. 1–6.

[27] S. J. Abram, J. C. Selinger, and J. M. Donelan, "Energy optimization is a major objective in the real-time control of step width in human walking," *J. Biomech.*, vol. 91, pp. 85–91, Jun. 2019.

[28] S. G. Bhat, S. Cherangara, J. Olson, S. Redkar, and T. G. Sugar, "Analysis of a periodic force applied to the trunk to assist walking gait," in *Proc. Wearable Robot. Assoc. Conf. (WearRAcon)*, Mar. 2019, pp. 68–73.

[29] K. Penke, K. Scott, Y. Sinskey, and M. D. Lewek, "Propulsive forces applied to the Body's center of mass affect metabolic energetics post-stroke," *Arch. Phys. Med. Rehabil.*, vol. 100, no. 6, pp. 1068–1075, Jun. 2019.

[30] P. Antonellis, S. Galle, D. De Clercq, and P. Malcolm, "Altering gait variability with an ankle exoskeleton," *PLoS ONE*, vol. 13, no. 10, 2018, Art. no. e0205088.

[31] S. Galle, P. Malcolm, S. H. Collins, and D. De Clercq, "Reducing the metabolic cost of walking with an ankle exoskeleton: Interaction between actuation timing and power," *J. NeuroEng. Rehabil.*, vol. 14, no. 1, p. 35, Dec. 2017.

[32] A. J. Young, J. Foss, H. Gannon, and D. P. Ferris, "Influence of power delivery timing on the energetics and biomechanics of humans wearing a hip exoskeleton," *Frontiers Bioeng. Biotechnol.*, vol. 5, pp. 1–4, Mar. 2017. [Online]. Available: https://www.frontiersin.org/article/10.3389/fbioe.2017.00004, doi: 10.3389/fbioe.2017.00004.

[33] A. M. Gonabadi, P. Antonellis, and P. Malcolm, "Development of waist perturbation effector for investigating relationship between mechanical work and metabolic cost," in *Proc. Dyn. Walking*, May 2018. [Online]. Available: https://youtu.be/W9rweEq0aFY

[34] P. Antonellis, A. M. Gonabadi, and P. Malcolm, "Effects of timing and magnitude of forward forces at the waist on the metabolic cost of walking," in *Proc. Int. Soc. Biomech./Amer. Soc. Biomech.*, Aug. 2019, p. 1355. [Online]. Available: https://www.dropbox.com/s/7xrlez4mcpjjn3z/isb2019_abstracts_all.pdf

[35] M. Saunders, V. Inman, and H. Eberhart, "The major determinants in normal and pathological gait," *J. Bones Jt. Surg.*, vol. 35, no. 3, pp. 543–558, 1953.

[36] G. A. Pratt and M. M. Williamson, "Series elastic actuators," in *Proc. IEEE/RSJ Int. Conf. Intell. Robots Syst.*, vol. 1. Aug. 1995, pp. 399–406.

[37] H. Vallery, J. Veneman, E. van Asseldonk, R. Ekkelenkamp, M. Buss, and H. van Der Kooij, "Compliant actuation of rehabilitation robots," *IEEE Robot. Autom. Mag.*, vol. 15, no. 3, pp. 60–69, Sep. 2008.

[38] J. Zhang and S. H. Collins, "The passive series stiffness that optimizes torque tracking for a lower-limb exoskeleton in human walking," *Frontiers Neurorobotics*, vol. 11, pp. 1–16, Dec. 2017.

[39] G. Brown, M. M. Wu, F. C. Huang, and K. E. Gordon, "Movement augmentation to evaluate human control of locomotor stability," in *Proc. 39th Annu. Int. Conf. IEEE Eng. Med. Biol. Soc. (EMBC)*, Jul. 2017, pp. 66–69.

[40] Y. Ding, M. Kim, S. Kuindersma, and C. J. Walsh, "Human-in-the-loop optimization of hip assistance with a soft exosuit during walking," *Sci. Robot.*, vol. 3, no. 15, Feb. 2018, Art. no. eaar5438.

[41] R. W. Jackson and S. H. Collins, "An experimental comparison of the relative benefits of work and torque assistance in ankle exoskeletons," *J. Appl. Physiol.*, vol. 119, no. 5, pp. 541–557, Sep. 2015.

[42] G. Pavei *et al.*, "Comprehensive mechanical power analysis in sprint running acceleration," *Scandin. J. Med. Sci. Sports*, vol. 29, no. 12, pp. 1892–1900, Dec. 2019.

[43] M. Kim, T. Chen, T. Chen, and S. H. Collins, "An ankle-foot prosthesis emulator with control of plantarflexion and inversion-eversion torque," *IEEE Trans. Robot.*, vol. 34, no. 5, pp. 1183–1194, Dec. 2018.

[44] K. A. Witte, J. Zhang, R. W. Jackson, and S. H. Collins, "Design of two lightweight, high-bandwidth torque-controlled ankle exoskeletons," in *Proc. IEEE Int. Conf. Robot. Autom.*, Jun. 2015, pp. 1223–1228.

[45] Y.-H. Chang and R. Kram, "Metabolic cost of generating horizontal forces during human running," *J. Appl. Physiol.*, vol. 86, no. 5, pp. 1657–1662, May 1999.

[46] A. H. Dewolf, Y. P. Ivanenko, R. M. Mesquita, F. Lacquaniti, and P. A. Willems, "Neuromechanical adjustments when walking with an aiding or hindering horizontal force," *Eur. J. Appl. Physiol.*, vol. 120, no. 1, pp. 91–106, Jan. 2020.

[47] J. Zhang, C. C. Cheah, and S. H. Collins, "Experimental comparison of torque control methods on an ankle exoskeleton during human walking," in *Proc. IEEE Int. Conf. Robot. Autom. (ICRA)*, May 2015, pp. 5584–5589.

[48] H. Vallery *et al.*, "Multidirectional transparent support for overground gait training," in *Proc. IEEE 13th Int. Conf. Rehabil. Robot. (ICORR)*, Jun. 2013, pp. 1–7.

[49] M. Nouri Damghani and A. Mohammadzadeh Gonabadi, "Numerical study of energy absorption in aluminum foam sandwich panel structures using drop hammer test," *J. Sandwich Struct. Mater.*, vol. 21, no. 1, pp. 3–18, Jan. 2019.

[50] M. Nouri Damghani and A. Mohammadzadeh Gonabadi, "Improving the Performance of the Sandwich Panel with the Corrugated Core Filled with Metal Foam: Mathematical and Numerical Methods," *Mech. Adv. Compos. Struct.*, vol. 6, no. 2, pp. 249–261, Nov. 2019.

[51] S. Qian, B. Zi, W. W. Shang, and Q. S. Xu, "A review on cable-driven parallel robots," *Chin. J. Mech. Eng.*, vol. 31, no. 4, p. 66, 2018.

[52] A. M. Grabowski and R. Kram, "Running with horizontal pulling forces: The benefits of towing," *Eur. J. Appl. Physiol.*, vol. 104, no. 3, pp. 473–479, Oct. 2008.

[53] J. R. Franz and R. Kram, "Advanced age affects the individual leg mechanics of level, uphill, and downhill walking," *J. Biomech.*, vol. 46, no. 3, pp. 535–540, Feb. 2013.

[54] G. A. Cavagna, "Force platforms as ergometers," *J. Appl. Physiol.*, vol. 39, no. 1, pp. 174–179, Jul. 1975.

[55] J. M. Donelan, R. Kram, and A. D. Kuo, "Simultaneous positive and negative external mechanical work in human walking," *J. Biomech.*, vol. 35, no. 1, pp. 117–124, Jan. 2002.

[56] M. Wu, T. G. Hornby, J. M. Landry, H. Roth, and B. D. Schmit, "A cable-driven locomotor training system for restoration of gait in human SCI," *Gait Posture*, vol. 33, no. 2, pp. 256–260, Feb. 2011.

[57] J. Rose, J. G. Gamble, A. Burgos, J. Medeiros, and W. L. Haskell, "Energy expenditure index of walking for normal children and for children with cerebral palsy," *Develop. Med. Child Neurol.*, vol. 32, no. 4, pp. 333–340, 1990.

[58] L. N. Awad, D. S. Reisman, R. T. Pohlig, and S. A. Binder-Macleod, "Reducing the cost of transport and increasing walking distance after stroke: A randomized controlled trial on fast locomotor training combined with functional electrical stimulation," *Neurorehabilitation Neural Repair*, vol. 30, no. 7, pp. 661–670, Aug. 2016.

[59] K. Scrivener, C. Sherrington, and K. Schurr, "Exercise dose and mobility outcome in a comprehensive stroke unit: Description and prediction from a prospective cohort study," *J. Rehabil. Med.*, vol. 44, no. 10, pp. 824–829, 2012.

[60] L. Marchal-Crespo and D. J. Reinkensmeyer, "Review of control strategies for robotic movement training after neurologic injury," *J. Neuroeng. Rehabil.*, vol. 6, no. 1, Dec. 2009.

[61] D. R. Louie and J. J. Eng, "Powered robotic exoskeletons in post-stroke rehabilitation of gait: A scoping review," *J. Neuroeng. Rehabil.*, vol. 13, no. 1, pp. 1–10, Dec. 2016.

[62] J. L. Patton, M. E. Stoykov, M. Kovic, and F. A. Mussa-Ivaldi, "Evaluation of robotic training forces that either enhance or reduce error in chronic hemiparetic stroke survivors," *Express Brain Res.*, vol. 168, no. 3, pp. 368–383, Jan. 2006.

[63] T. G. Hornby, D. D. Campbell, J. H. Kahn, T. Demott, J. L. Moore, and H. R. Roth, "Enhanced gait-related improvements after Therapist- versus robotic-assisted locomotor training in subjects with chronic stroke: A randomized controlled study," *Stroke*, vol. 39, no. 6, pp. 1786–1792, Jun. 2008.

[64] J. Hidler *et al.*, "Multicenter randomized clinical trial evaluating the effectiveness of the lokomat in subacute stroke," *Neurorehabil. Neural Repair*, vol. 23, no. 1, pp. 5–13, Jan. 2009.

[65] N. Giladi *et al.*, "Freezing of gait in patients with advanced Parkinson's disease," *J. Neural Transmiss.*, vol. 108, no. 1, pp. 53–61, 2001.

[66] K. K. Patterson *et al.*, "Gait asymmetry in community-ambulating stroke survivors," *Arch. Phys. Med. Rehabil.*, vol. 89, no. 2, pp. 304–310, Feb. 2008.

[67] D. S. Reisman, R. Wityk, K. Silver, and A. J. Bastian, "Locomotor adaptation on a split-belt treadmill can improve walking symmetry post-stroke," *Brain*, vol. 130, no. 7, pp. 1861–1872, 2007.

[68] B. R. Duffy, "Anthropomorphism and the social robot," *Robot. Auto. Syst.*, vol. 42, nos. 3–4, pp. 177–190, Mar. 2003.

[69] A. T. Asbeck, R. J. Dyer, A. F. Larusson, and C. J. Walsh, "Biologically-inspired soft exosuit," in *Proc. IEEE 13th Int. Conf. Rehabil. Robot. (ICORR)*, Jun. 2013, pp. 1–8.

[70] G. Stoquart, C. Detrembleur, and T. M. Lejeune, "The reasons why stroke patients expend so much energy to walk slowly," *Gait Posture*, vol. 36, no. 3, pp. 409–413, Jul. 2012.

[71] C. E. Mahon, D. J. Farris, G. S. Sawicki, and M. D. Lewek, "Individual limb mechanical analysis of gait following stroke," *J. Biomech.*, vol. 48, no. 6, pp. 984–989, Apr. 2015.

[72] F. Massaad, T. M. Lejeune, and C. Detrembleur, "Reducing the energy cost of hemiparetic gait using center of mass feedback: A pilot study," *Neurorehabil. Neural Repair*, vol. 24, no. 4, pp. 338–347, May 2010.

[73] A. M. Gonabadi, P. Antonellis, and P. Malcolm, "Differences between joint-space and musculoskeletal estimations of metabolic rate time profiles," *PLOS Comput. Biol.*, to be published.

[74] R. W. Jackson, C. L. Dembia, S. L. Delp, and S. H. Collins, "Muscle-tendon mechanics explain unexpected effects of exoskeleton assistance on metabolic rate during walking," *J. Exp. Biol.*, vol. 220, no. 11, pp. 2082–2095, 2017.

[75] B. R. Umberger, "Stance and swing phase costs in human walking," *J. Roy. Soc. Interface*, vol. 7, no. 50, pp. 1329–1340, Sep. 2010.

[76] P. Antonellis, C. M. Frederick, A. M. Gonabadi, and P. Malcolm, "Modular footwear that partially offsets downhill or uphill grades minimizes the metabolic cost of human walking," *Roy. Soc. Open Sci.*, vol. 7, no. 2, Feb. 2020, Art. no. 191527.

[77] C. Werner, G. P. Moustris, C. S. Tzafestas, and K. Hauer, "User-oriented evaluation of a robotic Rollator that provides navigation assistance in frail older adults with and without cognitive impairment," *Gerontology*, vol. 64, no. 3, pp. 278–290, 2018.

[78] G. Lee, T. Ohnuma, N. Young Chong, and S.-G. Lee, "Walking intent-based movement control for JAIST active robotic walker," *IEEE Trans. Syst., Man, Cybern. Syst.*, vol. 44, no. 5, pp. 665–672, May 2014.

[79] J. Kerestes and T. G. Sugar, "Enhanced running using a jet pack," in *Proc. 38th Mech. Robot. Conf.*, Aug. 2014, pp. 1–7.